CONF-960528--1

ROLE OF INTERFACES IN DEFORMATION AND FRACTURE:

TITANIUM ALUMINIDES*

M. H. Yoo and C. L. Fu

Metals and Ceramics Division
Oak Ridge National Laboratory
Oak Ridge, TN 37831, USA

Abstract

Available experimental data on deformation and fracture behavior of polysynthetically twinned (PST) TiAl crystals are analyzed on the basis of the calculated results of bulk and defect properties and shear fault, cleavage and interfacial energies of TiAl and Ti_3Al. The extent of dissociation width of an ordinary dislocation is calculated to be larger at α_2/γ and γ/γ interfaces by about two-fold as compared to the bulk of γ-phase, suggesting the enhanced slip along the interfaces when the crystal is at a soft orientation. Propagation of (111) cleavage cracks is influenced by the mixed mode (II and III) of external loading applied to the coplanar deformation twinning and ordinary slip, leading to translamellar fracture. According to the calculated interfacial fracture energies, cleavage cracking is to occur on α_2/γ boundaries and least likely on true-twin boundaries. Discussion is given on the roles of misfit dislocations, kinetics of dislocation-interface interactions, and hydrogen embrittlement in deformation and fracture processes.

*Research sponsored by the Division of Materials Sciences, U.S. Department of Energy, under contract number DE-AC05-96OR22464 with Oak Ridge National Laboratory, managed by Lockheed Martin Energy Research Corporation.

DISCLAIMER

Introduction

Microcomposite structures resulting from phase separation or decomposition can offer many unique microstructural advantages in thermodynamic stability, directional alignment, and fine dispersion of component phases. For examples, γ'/γ phases in Ni-base superalloys, α/β or β'/β in Ni-Al-X ternary (X = Cr or Ti) system, and α_2/γ in Ti-Al binary system are the outstanding cases in point. In the case of Ti-rich two-phase TiAl-Ti_3Al alloys, significant advances have been made recently in understanding the role of interfaces in deformation and fracture behavior of fully lamellar microstructure, due largely to controlled experimental investigations using the so-called polysynthetically twinned (PST) crystals, e.g., [1,2]. Quantitative interpretation of these experimental results, such as the anisotropic yield strength and tensile elongation [1,3] and fracture behavior [2,4] with respect to the lamellar orientation in PST TiAl crystals, requires fundamental information on the bulk and defect properties of the two constituent phases and the surface and interfacial energies of various γ/γ interfacial variants and α_2/γ boundary. It is this fundamental aspect of deformation and fracture in two-phase TiAl alloys which is the focus of this paper.

Phase stability and elastic constants [5-7], elastic incompatibility and misfit strain [8], bonding mechanisms [7,9], point defects in TiAl [9], shear fault energies [5,7], twin boundaries in TiAl [10], and cleavage and interfacial fracture energies [11,12] have been determined from total energy calculations using the full potential linearized augmented plane wave (FLAPW) method within the framework of the local density functional (LDF) theory. The purpose of this paper is to discuss available experimental data on the role of interfaces in deformation and fracture of PST TiAl crystals on the basis of the calculated results mentioned above [5-12].

Shear Fault Energies and Deformation Modes

TiAl

Plastic deformation of γ-TiAl by slip or twinning occurs primarily on {111} planes. Figure 1 (a) shows the atom stacking sequence on the (111) plane of the $L1_0$ structure viewed on the (111) plane, wherein the three different fault vectors, $\mathbf{b}_i$, are described. An ordinary dislocation is expected to dissociate into a pair of Shockley partials, with Burgers vectors of $\mathbf{b}_1 = [\bar{2}11]/6$ and $-\mathbf{b}_2 = [1\bar{2}1]/6$, forming a strip of complex stacking fault (CSF) ribbon,

$$[\bar{1}10]/2 \longrightarrow [\bar{2}11]/6 + \mathrm{CSF} + [\bar{1}2\bar{1}]/6\,. \qquad (1)$$

The four-fold dissociation of a superdislocation consists of two sets of $\mathbf{b}_3 = [11\bar{2}]/6$ and $-\mathbf{b}_2 = [1\bar{2}1]/6$ partial dislocations,

$$[01\bar{1}] \longrightarrow [11\bar{2}]/6 + \mathrm{SISF} + [\bar{1}2\bar{1}]/6 + \mathrm{APB} + [11\bar{2}]/6 + \mathrm{CSF} + [\bar{1}2\bar{1}]/6\ , \quad (2)$$

where SISF and APB are superlattice intrinsic stacking fault and anti-phase boundary, respectively. According to the classical Peierls concept of dislocation mobility, which says that the wider the planar dissociation configuration of a dislocation, the more mobile the dislocation is, the values of these fault energies provide a relative measure for the ease of gliding.

Ti_3Al

Plastic deformation of α_2-Ti_3Al of the $D0_{19}$ structure is known to occur by three slip systems, viz., the prism slip, $\{1\bar{1}00\}\langle 11\bar{2}0\rangle$, the basal slip, $(0001)\langle 11\bar{2}0\rangle$, and the pyramidal slip, $\{11\bar{2}1\}\langle 11\bar{2}\bar{6}\rangle$. The crystallographic aspects of the APB formation on these slip planes are well described by Umakoshi and Yamaguchi [13].

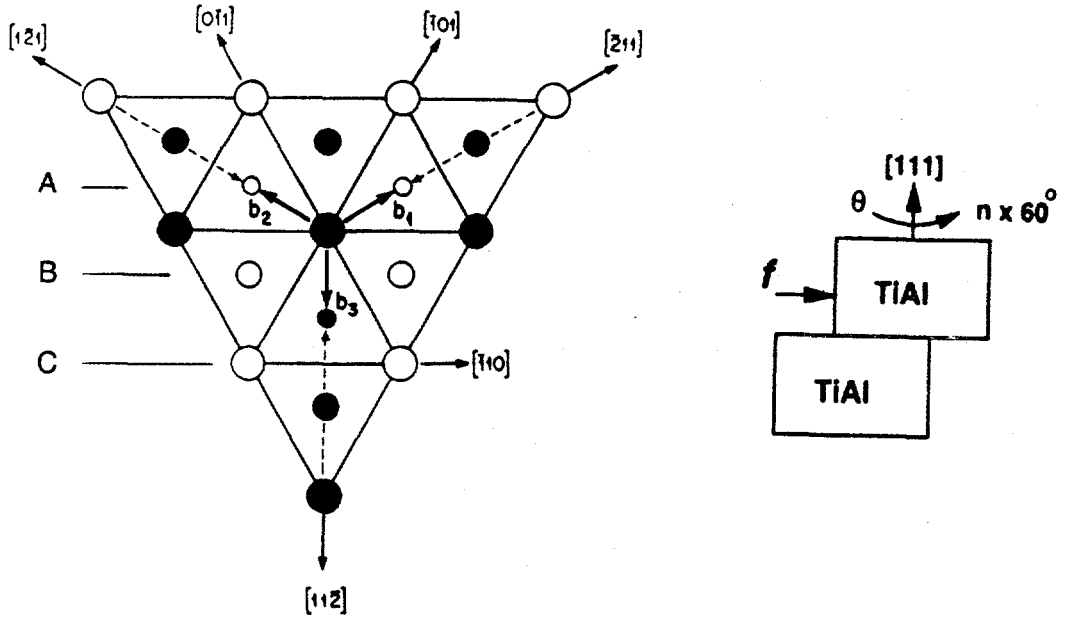

(a) (b)

Figure 1. (a) Atomic stacking (ABC) sequence on the (111) plane of the $L1_0$ structure, and (b) Schematic illustration of translation and rotation operations.

Structure and Energies of Interfaces

γ/γ Interfaces

Figure 1 (b) shows schematically how three different types of planar faults are created at three different types of γ/γ interfaces. When the angle of rotation, θ, and the fault shift vector, **f**, are both zero, the top and bottom halves together constitute the reference state of a single crystal, i.e., the total internal energy is set to zero.

All the calculated interfacial energies in Table I are the values obtained after atomic relaxation. Fault energies calculated for the three types on the (111) plane, i.e., APB with $\mathbf{f} = \mathbf{b}_1\text{-}\mathbf{b}_3$ or $\mathbf{b}_2\text{-}\mathbf{b}_3 = \langle\bar{1}01\rangle/2$, SISF with $\mathbf{f} = \mathbf{b}_3 = [11\bar{2}]/6$, and CSF with $\mathbf{f} = \mathbf{b}_1$ or $\mathbf{b}_2 = \langle\bar{2}11\rangle/6$, are listed in the first row (θ = 0). The APB, SISF, and true-twin boundary energies of $E_{APB} = 560$, $E_{SISF} = 90$, and $\Gamma_T = 60$ mJ/m^2, respectively, are similar to the results reported earlier [5]. It should be noted that in the earlier paper [5] the relaxation effect was included only for the APB. Since there is no change in the nearest-neighbor atomic coordination at the SISF, superlattice extrinsic stacking fault (SESF), and true-twin interfaces, atomic relaxation at these fault interfaces is assumed to be negligibly small. According to a more refined calculation, the present result gives an APB energy which is slightly increased from the previously reported value. With the inclusion of relaxation energy, the CSF energy is reduced from $E_{CSF} = 600$ mJ/m^2 to 530 mJ/m^2. Consequently, the hierarchy of the fault energies remains as $E_{CSF} \approx E_{APB} > E_{SISF} > E_{SESF} > \Gamma_T$, which is consistent with the recent experimental and simulation analysis in Ti-54at.%Al by Wiezorek and Humphreys [14].

Interfacial energies calculated for the three different types, i.e., pseudo-twin (θ = 60°), "rotational" (θ = 120°), and true-twin (θ = 180°) boundaries, are listed in the first column (**f** = 0) of Table I. The pseudo-twin boundary energy of $\Gamma_P = 300$ mJ/m^2 [10] is reduced to 270 mJ/m^2 after relaxation. At the pseudo-twin (θ = 60°) and rotational (θ = 120°) boundaries, while both E_{APB} and E_{CSF} are reduced markedly, by factors of about two, as compared to those in the bulk, E_{SISF} is increased by a factor of three. At the true-twin boundary, on the other hand, changes in the fault energies are relatively small, with slight increases in both E_{APB} and E_{CSF} and a decrease in E_{SISF}.

Table I. Interfacial Energies of γ/γ Lamellar Boundaries in TiAl (in Units of mJ/m^2)

Interface type	θ	$\mathbf{f}=0$ Γ_i	$\frac{1}{2}<\bar{1}01]$ APB	$\frac{1}{6}[11\bar{2}]$ SISF	$\frac{1}{6}<\bar{2}11]$ CSF
Bulk	0	0	560	90	530
Pseudo-twin	60°	270	270	270	270
Rotational	120°	250	250	280	280
True-twin	180°	60	550	60	550

Degeneracies of fault energies noted in Table I are due to geometrically equivalent characteristic patterns of interfaces resulting from certain combinations of rigid-body translations and rotations according to the O-lattice theory [15]. An example of these degeneracies can be described with the aid of Fig. 2, where the C-layer of atoms have been rotated and translated with reference to the B-layer. Figure 2(b) shows the geometric pattern of interfaces by $\theta = 60°$ and $\mathbf{f}= 0$, and Fig. 2(c) shows that by $\theta = 60°$ and $\mathbf{f} = \mathbf{b}_2$. These two operations result in a geometrically equivalent pattern between two atomic rows of the adjacent B and C layers. Because of the assumption that c/a = 1, the magnitude of $\mathbf{b}_1 = \mathbf{b}_2$ are equal to that of $\mathbf{b}_3$, and the atomic lattices shown in Figs. 1 and 2 are equilateral triangles. With the actual value of c/a = 1.02 for γ-TiAl, this symmetry and the degeneracies are broken, thus giving rise to long-range coherency stresses and interfacial dislocations to accommodate the misfit strain across the interface. A contribution of misfit dislocation content to the determination of interfacial fracture energy is discussed below.

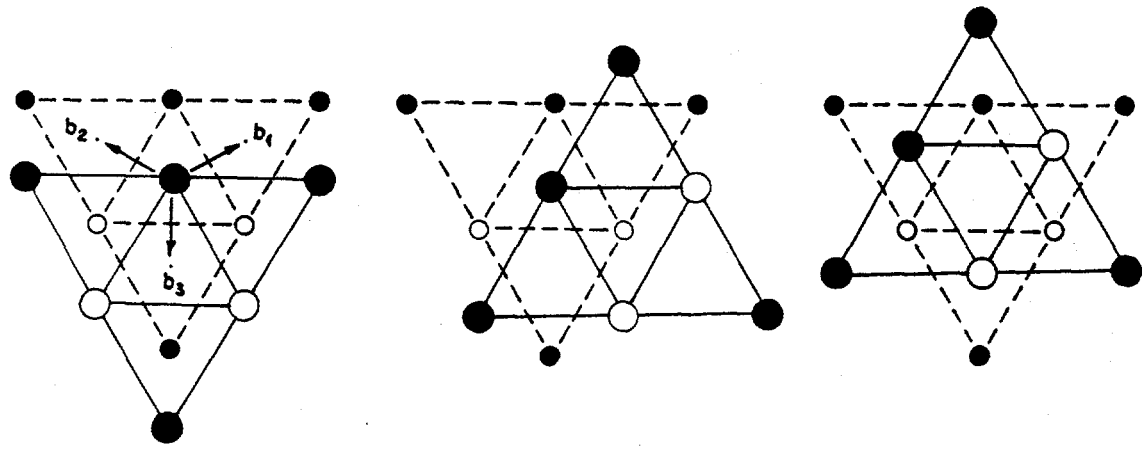

Figure 2. Degeneracy of the shear faults at a pseudo-twin interface, (a) reference state. (b) $\theta = 60°$, $\mathbf{f} = 0$, and (c) $\theta = 60°$, $\mathbf{f} = \mathbf{b}_2$

<u>α_2/γ Interface</u>

At an α_2/γ interface with the crystallographic habit relationship of $(0001)[11\bar{2}0]$-Ti_3Al and $(111)[1\bar{1}0]$-TiAl, the interfacial energy is calculated to be 100 mJ/m^2 (the reference energy in this case is the sum of TiAl and Ti_3Al bulk energies). Significant reductions of E_{APB} and E_{CSF} in α_2 phase to those (280 and 220 mJ/m^2, respectively) at the Ti_3Al/TiAl interface were reported recently [7], which are summarized in Table II.

Table II. Calculated Shear Fault Energies at the TiAl/Ti_3Al Interface (in Units of mJ/m^2)

Plane	APB	SISF	CSF
(111) TiAl	560	90	530
(0001) Ti_3Al	300		320
TiAl/Ti_3Al	280	20	220

Inhomogeneous Slip and Plastic Anisotropy

Possible roles of various interfaces in the slip system, $\{111\}\langle 1\bar{1}0]/2$, can be discussed with the aid of Figure 3 which schematically illustrates true-twin (TT, γ_1/γ_2), pseudo-twin (PT, γ_1/γ_3), rotational (RB, γ_1/γ_4), and α_2/γ (Ti_3Al/TiAl) boundaries. Domain boundaries of other γ/γ-type that are roughly perpendicular to the (111) plane are neglected here for simplicity. The crystallographic orientation shown in Fig. 3 is with reference to the γ_1 domain. A screw ordinary dislocation of Burgers vector, $[1\bar{1}0]/2$, is dissociated on either the (111) or $(\bar{1}\bar{1}1)$ slip plane according to Eq. (1), where $E_{CSF} = 530\ mJ/m^2$ in the γ_1 bulk gives the equilibrium width of w = 0.23 nm [16]. The calculated values of E_{CSF} at the γ/γ-type interfaces (the last column of Table I) and at the α_2/γ interface [7] are shown in Fig. 3, which schematically depicts relatively wider dissociations at interfaces, the widest being at the α_2/γ interface with $w \approx 0.55$ nm. According to the simple criterion for the ease of gliding that the wider the dissociation configuration of a dislocation, the more mobile the dislocation is [16], the mobility of $[1\bar{1}0]/2$ screw dislocation is expected to be slightly reduced along a true-twin boundary, but significantly enhanced along all other types of the interfaces.

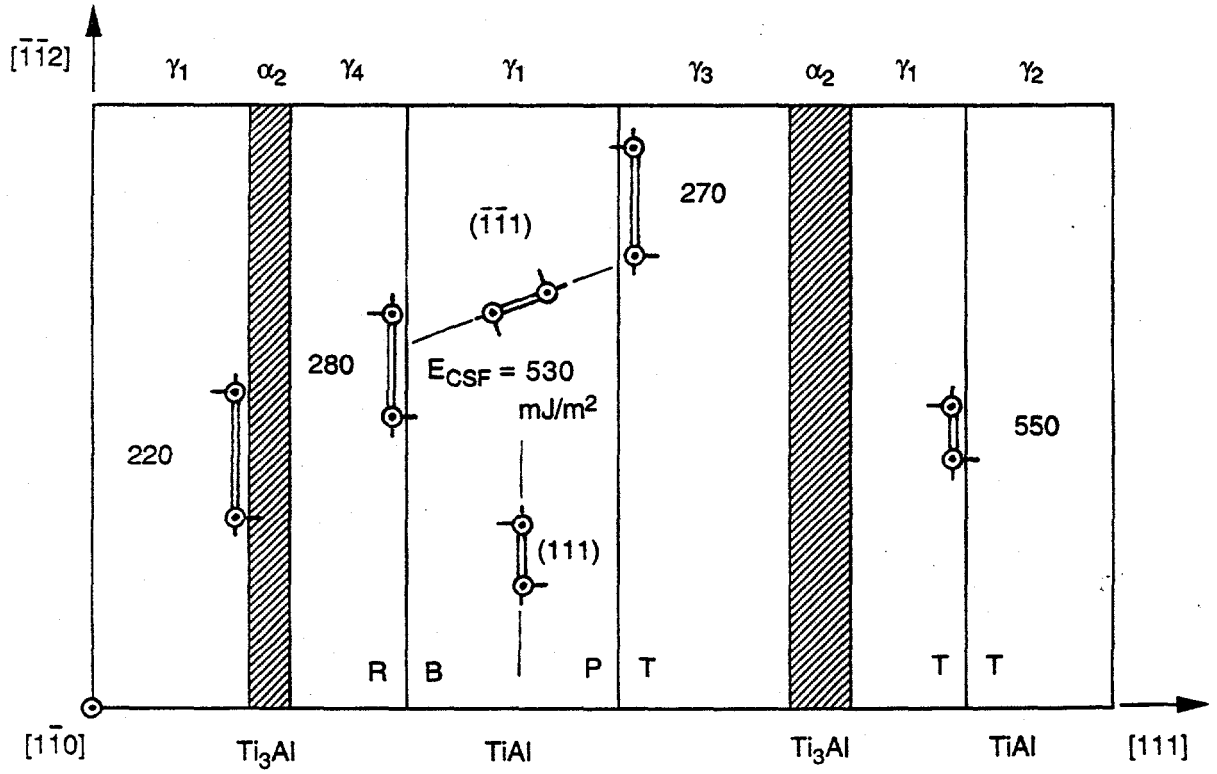

Figure 3. CSF energies and dissociation of screw $[1\bar{1}0]/2$ dislocations in PST crystals.

Because of more complex dissociation configuration involving all three types of the planar faults, Eq. (2), the role of interfaces in the relative mobility of superdislocations is more complicated than of ordinary dislocations. As listed in Table I, while E_{APB} and E_{CSF} in the bulk of γ-phase are both reduced, by about a half, at pseudo-twin and 120° rotational boundary interfaces, E_{SISF} is increased about threefold.

As far as ordinary dislocations are involved, the enhanced mobility along these lamellar interfaces supports the notion of "channeled dislocation motion" [17] or "supersoft deformation mode" [15] in lamellar TiAl, which may be a contributing factor to the strong orientation dependence of yield strength in PST TiAl crystals [1]. The recent experiment purported to examine the role of α_2/γ interfaces in plastic deformation at the soft orientation (shear parallel to the lamellar interfaces) revealed, however, that plastic shear strain occurred mostly away from the α_2/γ interfaces [3]. Though Inui et al. [3] concluded that shear strain in the soft orientation was due to twinning and slip in the bulk of γ lamellae, possibility of inhomogeneous flow by ordinary dislocations along γ/γ interfaces cannot be ruled out from this experimental observation. Presumably, misfit dislocations and ledges on an α_2/γ interface significantly influence the parallel slip process along the interface.

Cleavage and Interfacial Fracture

Once a cleavage crack is initiated on a (111) plane, which is of the lowest cleavage energy in TiAl [8], it may propagate across a series of γ/γ interfaces under the influence of mode-II and mode-III components of external loading applied to the coplanar $(111)[11\bar{2}]$ twinning (edge) and $(111)[1\bar{1}0]$ ordinary slip (screw), leading to translamellar fracture. This effect of mode mixity was illustrated in terms of crack-tip stress fields [8] and observed in an electron microscopy study [18].

Using the ideal cleavage energies, G_c, calculated earlier [8] and the interfacial energies, Γ_i, obtained recently [12], one can evaluate interfacial fracture energy by using the relationship,

$$G_i = G_c - \Gamma_i - E_m, \qquad (3)$$

where E_m is the misfit energy estimated using the Frank and van der Merwe method [19] and the calculated lattice parameters of TiAl and Ti_3Al [5-7]. The calculated results are summarized in Table III. Because of the approximations involved in determining the interfacial and misfit energies, the final interfacial fracture energies are only estimates. Nevertheless, these results enable us to set a relative measure of interfacial fracture mode, indicating that fracture is easiest along α_2/γ boundaries and most difficult along true-twin boundaries.

Table III. Interfacial Fracture Energies in Two-Phase TiAl
(in Units of J/m^2)

Interface	G_c	Γ_i	E_m	G_i
γ/γ				
PT (60°)	4.5	0.27	(int.)	~4.1
RB (120°)	4.5	0.25	0.26	4.0
TT (180°)	4.5	0.06	(low)	~4.4
α_2/γ	4.65	0.10	0.73	3.8

According to the calculated interfacial fracture energies (Table III), cleavage cracking is least likely to occur on true-twin boundaries and most likely on α_2/γ boundaries. This is consistent with the recent experimental findings of three-point bending tests of Chevron-notched PST crystals of TiAl [4]. In the fracture tests using microcompact tension specimens of TiAl PST crystals [2], it was found that a microcrack was initiated on the α_2 plate and easily developed into a main crack on the (0001) plane, finally leading to failure because of the hydrogen embrittlement of the α_2 phase. Though the intrinsic cleavage energy of the (0001) plane in the α_2 phase is, G_c = 4.8 J/m^2 [8], higher than those of any other interfaces listed in Table III, it could be reduced appreciably, below the value of 3.8 J/m^2, due probably to the relatively high solubility of interstitials (hydrogen, in this case) in the α_2 phase.

Figure 4 shows a schematic diagram illustrating the experimental results by Oh et al. [20] on the fracture mode changes in PST crystals in response to the applied strain rate under a hydrogen producing environment. When the strain rate was $\dot{\varepsilon} = 2 \times 10^{-4}$ s^{-1}, the fracture mode was an interlamellar type along the (111) γ/γ interfaces parallel to the α_2/γ interfaces as shown by Fig. 4 (a), and the tensile elongation was 16%. When the strain rate was raised to $\dot{\varepsilon} = 1 \times 10^{-1}$ s^{-1}, the fracture mode was changed to a translamellar type, Fig. 4 (b), which occurred with nearly a factor of two increase in ductility of ε_f = 30%. The authors [20] concluded that (a) the interfacial (γ/γ with θ = 60° and 120°) cleavage was initiated due to the reduced interfacial energy by hydrogen segregation, and (b) at the higher strain rate diffusion time for the atomic hydrogen was too short to effect the interlamellar fracture.

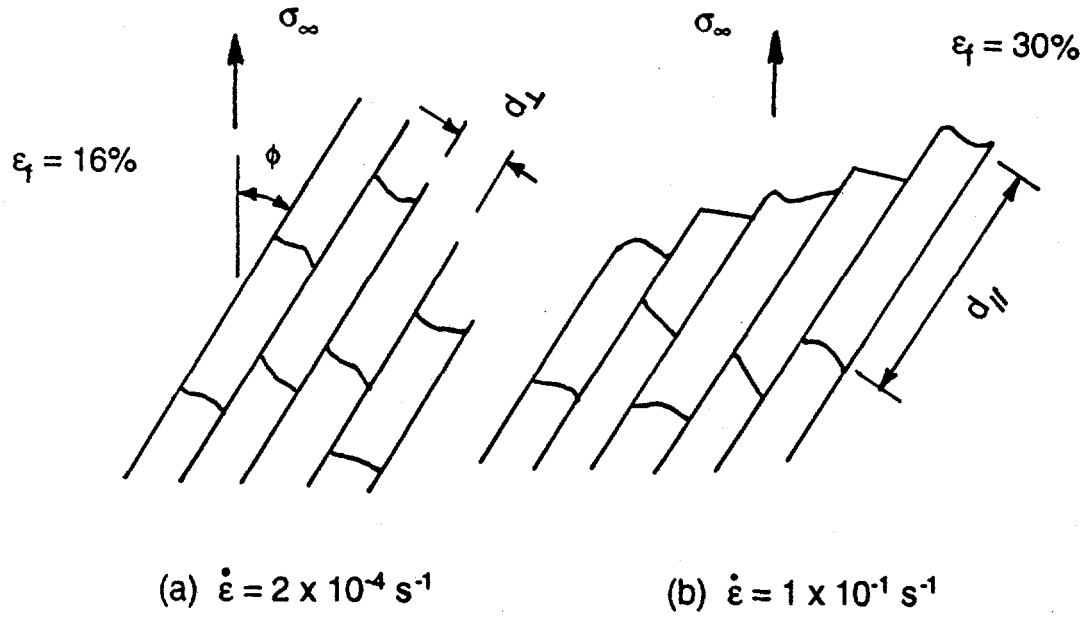

Figure 4. Schematic illustration (based on Ref. [20]) of fracture mode change in PST crystals (ϕ = 31°) with two different strain rates under environmental embrittlement at room temperature.

Two additional viewpoints regarding interpretation of these experimental results [20] were offered based on the energetic and kinetic aspects of nucleation and propagation of cracks [21]. First, in Fig. 4 (a), once nucleated, the propagation of an interfacial crack can be promoted by the mixed-mode (I+II) effect, together with the enhanced slip along the interface. Second, in Fig. 4 (b), because of the relatively large interspacing of the γ/γ domain boundaries, $d_{//}$, as compared to the average interlamellar spacing, $d_{\perp}$, translamellar crack nucleation at a γ/γ domain boundary may occur due to a pile-up of soft-mode ordinary dislocations under the high strain rate.

Discussion

The ratio of γ/γ-type interfacial energies calculated for true-twin, pseudo-twin, and rotational boundaries ($\Gamma_T : \Gamma_P ; \Gamma_R$) is 1 : 4.5 : 4.2. This is consistent with more frequent observation of true-twin type lamellar interfaces, in two-phase TiAl alloys of binary compositions, compared with the 120°-rotational and pseudo-twin types [22]. On the other hand, the reason why the lamellar domain boundaries of higher energies than that of the true-twin type, by factors of more than four, do appear in the TiAl phase is not entirely clear. One possible explanation for the formation of these lamellar domain boundaries may be closely related to the preexisting anti-phase domain boundaries (APBs) of Ti_3Al before the $\alpha_2 \rightarrow \alpha_2 + \gamma$ transformation [23].

Misfit dislocations present at semicoherent α_2/γ and γ/γ interfaces are often the sites for generation of slip dislocations and deformation twinning [24]. When a dislocation pile-up occurs against an interface, stress concentration at the interface may reach a level sufficiently high for either initiation of slip or twinning into the adjacent domain leading to a Hall-Petch type relationship, or crack nucleation by the Stroh mechanism. Using Hall-Petch and Stroh mechanisms, Hazzledine and Kad [25] discussed the orientation dependent yield and fracture stresses reported in PST TiAl crystals [1]. In light of the fact that all the deformation modes in γ-TiAl occur on {111} planes and the ideal cleavage energy is lowest on these planes, the importance of mode-mixity was emphasized earlier not only in crack-tip plasticity, but also in nucleation of slip, twinning, or cracking by stress concentration due to a dislocation pile-up [8].

Most of modeling analyses for the stress concentration associated with a pile-up of dislocations, including the above two papers [8,25], are based on a static equilibrium condition, and as such these cannot be applied to treat dynamic or quasi-static aspects of deformation and fracture processes. Regarding the stress concentration associated with a dislocation pile-up against an interface, the role of energetic barriers estimated on the basis of linear elasticity is relatively unimportant as compared to that of kinetics of the dislocation reaction resulting from the leading dislocation [21]. In other words, how efficiently the reaction products (resulting from incorporation of a slip dislocation into a semicoherent interface containing interfacial dislocations) glide/climb away from the site of intersection is far more crucial to whether or not the following dislocations can be incorporated into the interface. This kinetic barrier of slip-interface interaction will be lowered with increasing temperature, which may be one of the reasons for a sharp drop in the yield stresses for the hard ($\phi = 0°$ and $\phi = 90°$) orientations [3]. Another possible contribution to the softening at elevated temperatures (> 1073 K) may be from deformation twinning in non-stoichiometric Ti_3Al alloy at the elevated temperatures [26].

According to the recent review by Wiezorek and Humphreys [14], the hierarchy of planar fault energies in Ti-54%Al is $E_{CSF} > E_{APB} > E_{SISF}$, and the values for TiAl are $E_{APB} > 250$ mJ/m^2 and $E_{SISF} = 140$ mJ/m^2. Our calculated results of $E_{APB} = 560$ mJ/m^2 and $E_{SISF} = 90$ mJ/m^2 for TiAl (at stoichiometry) at 0K indicate that temperature and composition dependencies of planar fault energies in TiAl may be very substantial. Further theoretical and experimental studies are needed to assess the dependencies of planar fault energies on temperature and composition in order to better understand the role of interfaces in mechanical behavior of Ti-rich two-phase alloys.

Summary

The intrinsic values of interfacial energies based on first-principles calculations, including atomic relaxation, were obtained for the three types of γ/γ interfaces and the α_2/γ lamellar boundary in two-phase TiAl alloy. The pseudo-twin boundary energy is highest, $\Gamma_P = 270$ mJ/m^2, and the true-twin boundary energy is lowest, $\Gamma_T = 60$ mJ/m^2. Planar fault energies at pseudo-twin and 120° rotational interfaces are markedly different from those in the bulk of γ-phase, i.e., approximately, E_{APB} and E_{CSF} decreases by a half and E_{SISF} increases by a threefold. Enhanced mobility of ordinary dislocations along α_2/γ and γ/γ interfaces (except true twin boundaries) is predicted based on the reduced E_{CSF} values. Interfacial fracture energies are estimated to be highest for the true-twin boundary and lowest for the α_2/γ lamellar boundary. Crack nucleation at γ/γ domain boundaries and the mode mixity together with the enhanced slip along the interfaces are suggested as contributing factors involved in the reported environmental embrittlement effects on PST TiAl crystals.

References

1. T. Fujiwara, A. Nakamura, M. Hosomi, S. R. Nishitani, Y. Shirai, and M. Yamaguchi, "Deformation of PST Crystals of TiAl with a Nearly Stoichiometric Composition," Phil. Mag. A **61** (1990), 591-606.

2. T. Nakano, T. Kawanaka, H. Y. Yasuda, and Y. Umakoshi, "Effect of Lamellar Structure on Fracture Behavior of TiAl PST Crystals," Mater. Sci. Eng. A **194** (1995), 43-51.

3. H. Inui, K.Kishida, M. Misaki, M. Kobayashi, Y. Shirai, and M. Yamaguchi, "Temperature Dependence of Yield Stress, Tensile Elongation and Deformation Structures in PST Crystals of TiAl," Phil. Mag. A **72** (1995), 1609-1631.

4. S. Yokoshima and M. Yamaguchi, "Fracture Behavior and Toughness of PST Crystals of TiAl," Acta Mater. **44** (1996), 873-883.

5. C. L. Fu and M. H. Yoo, "Elastic Constants, Fault Energies, and Dislocation Reactions in TiAl: A First-Principles Total-Energy Investigation," Phil. Mag. Lett. **62** (1990), 159-165.

6. J. Zou, C. L. Fu, and M. H. Yoo, "Phase Stability of Intermetallics in the Al-Ti System: A First-Principles Total-Energy Investigation," Intermetallics **3** (1995) 265-269.

7. C. L. Fu, J. Zou, and M. H. Yoo, "Elastic Constants and Planar Fault Energies of Ti_3Al and Interfacial Energies at the Ti_3Al/TiAl Interface by First-Principles Calculations," Scr. Metall. Mater. **33** (1995), 885-891.

8. M. H. Yoo, J. Zou, and C. L. Fu, "Mechanistic Modeling of Deformation and Fracture Behavior in TiAl and Ti_3Al," Mater. Sci. Eng. A **192/193** (1995), 14-23.

9. C. L. Fu and M. H. Yoo, "Bonding Mechanisms and Point Defects in TiAl," Intermetall. **1** (1993), 59-63.

10. M. H. Yoo, C. L. Fu, and J. K. Lee, "Elastic Properties of Twin Dislocations in Titanium Aluminides," Twinning in Advanced Materials, ed. M. H. Yoo and M. Wuttig, (TMS Symp. Proc., Warrendale, PA, 1994), 97-106.

11. M. H. Yoo and C. L. Fu, "Cleavage Fracture of Ordered Intermetallic Alloys," Mater. Sci. Eng. A **153** (1992), 470-478.

12. C. L. Fu and M. H. Yoo, "Interfacial Energies in Two-Phase TiAl-Ti_3Al Alloy," Scr. Mater. (submitted).

13. Y. Umakoshi and M. Yamaguchi, "The Stability and Energies of Planar Faults in DO_{19} Ordered Structure," Phys. Stat. Sol. (a) **68** (1981), 457-468.

14. J.M.K. Wiezorek and C. J. Humphreys, "On the Hierarchy of Planar Fault Energies in TiAl," Scr. Metall. Mater. **33** (1995), 451-458.

15. S. Rao, C. Woodward, and P. M. Hazzledine, "The Interaction between Dislocations and Lamellar Grain Boundaries in PST γ-TiAl," Defect-Interface Interactions; ed. E. P. Kvam, A. H. King, M. J. Mills, T. D. Sands, and V. Vitek, (MRS Symp. Proc. Vol. 319, Pittsburgh, PA, 1994), 285-292.

16. M. H. Yoo and C. L. Fu, "Strength of Intermetallic Compounds: TiAl," Intermetallic Compounds for High-Temperature Structural Applications, ed. M. Yamaguchi and H. Fukutomi, (Proc. 3rd Japan Int. SAMPE Symp., 1993), 1286-1293.

17. B. K. Kad, P. M. Hazzledine, and H. L. Fraser, "Lamellar Interfaces and Their Contribution to Plastic Flow Anisotropy in TiAl-Based Alloys," High-Temperature Ordered Intermetallic Alloys V, ed. I. Baker, R. Darolia, J. D. Whittenberger, and M. H. Yoo, (MRS Symp. Proc. Vol. 288, MRS, Pittsburgh, PA, 1993), 495-500.

18. F. Appel, U. Christoph, and R. Wagner, "An Electron Microscope Study of Deformation and Crack Propagation in ($\alpha_2+\gamma$) Titanium Aluminides," Phil. Mag. A **72** (1995), 341-360.

19. J. W. Mathews, "Misfit Dislocations in Screw Orientation," Phil. Mag. **29** (1974), 797-802.

20. M. H. Oh, H. Inui, M. Misaki, and M. Yamaguchi, "Environmental Effects on the Room Temperature Ductility of PST Crystals of TiAl," Acta Metall. Mater. **41** (1993), 1939-1949.

21. M. H. Yoo, "Time-Dependent Stress Concentration and Microcrack Nucleation in TiAl," Int. Symp. on Gamma Titanium Aluminides, ed. Y.-W. Kim, R. Wagner, and M. Yamaguchi, (TMS Symp. Proc., Warrendale, PA, 1995), 259-266.

22. D. M. Dimiduk, Y. Sun, and P. M. Hazzledine, "Interfacial Structure and Lattice Mismatch in Lamellar TiAl Alloys," High-Temperature Ordered Intermetallic Alloys VI, ed. J. H. Horton, I. Baker, S. Hanada, R. D. Noebe, and D. S. Schwartz, (MRS Symp. Proc. Vol. 364, Pittsburgh, PA, 1995), 599-604.

23. Y. S. Yang and S. K. Wu, "Orientation Faults of γ Lamellae in a Ti-40%Al Alloys," Scr. Metall. Mater. **25** (1991), 255-260.

24. F. Appel, P. A. Beaven, and R. Wagner, "Deformation Processes related to Interfacial Boundaries in Two-Phase γ-Titanium Aluminides," Acta Metall. Mater. **41** (1993), 1721-1732.

25. P. M. Hazzledine and B. K. Kad, "Yield and Fracture of Lamellar γ/α_2 TiAl Alloys," Mater. Sci. Eng. A **192/193** (1995), 340-346.

26. J. W. Lee, S. Hanada, and M. H. Yoo, "Deformation Twinning in Non-Stoichiometric Ti_3Al Alloys," Scr. Metall. Mater. **33** (1995), 509-514.

Note: Recently, after the completion of this manuscript, the authors learned of the experimental results by Kad and Asaro (unpublished research, University of California, San Diego) on deformation inhomogeneities in PST-TiAl crystals. They observed γ/γ interface sliding in PST-TiAl deformed in compression at room temperature by means of offset displacement of the fiducial lines. In addition to this evidence of coarse slip parallel to the laminates, localized at the γ/γ and/or α_2/γ interfaces, they also observed transition from the coarse slip to mode II cracking parallel to lamellar interfaces, and then to mixed mode (I+II) across the interfaces. These experimental findings are entirely consistent with the present results predicting inhomogeneous slip along the lamellar interfaces (60° pseudo-twin and 120° rotational γ/γ, and α_2/γ) and translamellar crack nucleation due to a pileup of soft mode ordinary dislocations.